Study the Antifungal Activity of ZnS:Mn Nanoparticles Against Some Isolated Pathogenic Fungi

IOP Conf. Series: Journal of Physics: Conf. Series **1178** (2019) 012008 doi:10.1088/1742-6596/1178/1/012008

Study the Antifungal Activity of ZnS:Mn Nanoparticles Against Some Isolated Pathogenic Fungi

Batol I. Dheeb[1], Sundus M. A. Al-dujayli[2], Isam M. Ibrahim[2], Qayes A. Abbas[3], Ahmed H. Ali[4], Asmeit Ramizy[5], M.H. Eisa[6], A.I. Aljameel[7], Iftikhar M. Ali[2], Basim Mohammed Khashman [8], Anaam F. Hussain[9]

[1] Dept of Pathological Analysis, College of Applied Science, Samarra University, Samarra, Iraq.
[2] Dept of phys, College of science, Baghdad University, Baghdad, Iraq.
[3] Dept of Phys, College of Education for Pure Science, University of Anbar, Iraq.
[4] Dept. of Medical Phys., College of Applied Sciences, University of Fallujah, Iraq
[5] Dept of phys, College of Science, University of Anbar, Anbar, Iraq
[6] Dept of phys, College of Science, Sudan University of Science Technology, Khartoum, Sudan
[7] Dept of phys, College of Science, Al Imam Mohammad Ibn Saud Islamic University, Riyadh, Saudi Arabia
[8] Iraqi National Cancer Research Center (INCRC), Baghdad, Iraq.
[9] Dept of Biology, College of science, Dayala University, Dayala, Iraq.

Abstract

An aqueous chemical reaction has been used to prepare antifungal ZnS: Mn nanostructures, from manganese chloride, zinc acetate and thioacetamide in aqueous solution. The nanoparticle size has been controlled using thioglycolic acid as a capping factor. The major feature of the ZnS:Mn nanoparticles of average diameter ~ 2.73 nm is that possible preparing the sample from sources non-toxic precursors. The manufactured ZnS:Mn nanoparticles were identified and characterized to investigate the structure, morphology, composition of components of the nanoparticles and optical properties using (XRD, SEM, EDS and UV-Vis spectroscopy) techniques respectively. The agar dilution mechanism used to evaluate of the antifungal activity using ZnS:Mn nanoparticles which showed an efficient antifungal activity against four fungal models *Aspergillus fumigatus ,Aspergillus falvus, Trichophyton mentagrophyte, and Microsporum audonii* the inhibition increase with the increase of nanoparticle concentration. The antifungal property of manganese doped zinc sulphide nanoparticles creates from the interaction between nanoparticles and water led to generation the interactive oxygen species. Perturbation of the cell membranes due to the existence of Zn ions and S affecting on inhibition rate . the study aimed to evaluation the Antifungal Activity of ZnS:Mn Nanoparticles Against Some Isolated Pathogenic Fungi.

Keywords: Antifungal activity, nanoparticles, co-precipitation method*, Aspergillus,Trichophyton*

Introduction

Antifungal activity of nanoparticles has been effectively evinced in present times for a great variety of antifungal applications. In the first, using of nanoparticles as antimicrobial and antibacterial agents has become effective and developed according to (1-5) although the difficulty of domination the microbial growth because of the presented resistance by microbes against traditional antimicrobial agents. Many of mechanisms are assumed to clarify the antibacterial influence of nanoparticles. Mechanism produce reactive oxygen species (ROS) during photo induced has been an eminent reason antimicrobial Capability

which found in nanoparticles of ZnO as well as TiO_2 (2, 3, 6, 7). Another mechanism has been reported which is the influence of particle size on microbes and it is found that the antimicrobial activity increases depending on decreasing of the size of particles (8-10). While others observed that an efflux mechanism which leads to emission of ions in particular cases (11-13). In the previous studies, many efforts have done on metal oxide nanosized particles, recently there are plentiful researches relating to the antibacterial effect of zinc sulphide (14, 15). It found that due to the effect of quantum confinement, ZnS nanoparticles originate from chemical precipitation techniques have band gap more than 3.6 eV which different from the bulk ZnS particles. Additionally, it has been found that doping by metallic ions such as Ni and Ag made a shift in the band gap for these nanoparticles to improve their effective properties (15, 16) and this leads to presence of energy levels resulted by the impurity in the crystalline structure. Photocatalytically effective ZnS nanoparticles formed by microwave irradiation were affected by doping with Silver. This doping leads to an increasing in the photocatalytic activity and leads to phase transition of ZnS structure (15). Doping of Nanocrystalline ZnS, manufactured by ultrasonic spray pyrolysis, with Ni created new levels in the band energy of the crystal and owing to their excellent crystallinity and high surface area, the photocatalytic effectiveness of these nanoparticles for H_2 production and effectively utilized beneath visible light ray (16). Considerable efforts were made to study the antimicrobial activity of ZnS nanoparticles as a photocatalyst by photoactive mechanisms leads to be attractive material to use in antimicrobial systems (14, 15). The other important use of nanoparticles was as antifungal agents. The antifungal activity of Ag nanosized particles which used as antifungal drug carried out on two samples of yeasts; *Candida albicans* and *Saccharomyces cerevisiae*. Ag nanoparticles showed an efficient antifungal activity for fungal samples investigated (17).

The most common opportunistic infections caused from fungi lead to effect human by particular situations like immune impairment, gestation and some diseases as well as the animals and plants (18) may affect by these infections. Although, Antifungal drug treatment is one of therapies which gave antifungal drug resistance but it is appeared not a same as the issue in bacteria as antibacterial agents, the limitation of availability of therapy comes from the number of kinds of antifungal agents (19). This has led to attention to search about new antifungal agents. Therefore, the main focus of this study, is to study the antifungal properties of nano ZnS:Mn particles. In this work, we report the use of ZnS:Mn nanoparticles, synthesized by an chemical co-precipitation technique, for antifungal activity against four fungal strains.

Materials & Methods

Chemical compounds: Chemical compounds: Manganese chloride , zinc acetate, and thioacetamide were purchased from Merck chemical company, Germany.

Characterization of ZnS:Mn semiconductor nanoparticles

The prepared sample was characterized using X-ray diffraction (SHIMADZU-XRD 6000) used a Cu Kα radiation at λ=1.5406Å (2Θ = **20˚-60˚**, scan speed = 0.2 s/step, increment = 0.02, operating voltage = 40 kV and operating current = 40 mA). The phase purity and the average particle size were determined for the sample. The nanophase was specified through compare the intensities and peak positions. The morphological properties of sample surfaces have been investigated, field emission scanning electron micrograph (FESEM) and energy dispersive spectroscopy (EDS) used to examine the surface structures, also carried out to attain the composition. UV- Visible SP 8001 spectrophotometer was used to gauge the optical absorbance spectra along the domain 190–1100 nm. The optical measurement was carried out on the powder which was firstly dispersed in distilled water and lay in a quartz cuvette. Basically, as a reference specimen of measuring used the distilled water.

Isolation and identification of fungal isolates

All fungal isolates were obtained from the laboratories of the Biotechnology Department, College of Science in Baghdad University. All the organisms were confirmed using some test within the laboratory staff (20). Table (1) show the Clinical fungal isolates and their sources.

Table 1. Clinical fungal isolates and their sources

Fungus Species	Sources of Isolation
Aspergillus fumigatus	Lower respiratory tract infection
Aspergillus flavus	Lower respiratory tract infection
Trichophyton mentagrophytes	Dermal infection : skin
Microsporum audouinii	Dermal infection: skin

Method of preparation of *ZnS:Mn* nanoparticles

Preparation has been done by using zinc acetate dihydrate, manganese chloride dihydrate and thioacetamide, in a chemical reaction in solutions to produce Zn, S and Mn. In an exemplary chemical composition, 5mM of zinc acetate dihydrate, 0.1mM of manganese chloride dehydrate and 6mM of thioacitamide have been stirred for half an hour individually. Firstly, the solution of manganese chloride dehydrate has been added to the zinc acetate dihydrate, during the *continuous* stirring, and then added a drop from thioacetamide solution to the eventual solution with *continuous* stirring for half an hour. After that, a quantity of thioglycolic acid (0.2M), as a capping factor, was added to the above solution and stirring them for 2h at 100 °C. As a result of the interaction, ZnS has been obtained as a whitey yellow deposition. Surplus amount of water was utilized to washing the finished product to strip any non-reactive species as well as drying oven at 60 °C for 5 hours was used to dry the product. After adequate drying, mortar and pestle was used to smashing the precipitate to accurate powder, this procedure is mentioned in previous work (21).

Concentrations of ZnS:Mn compound

Dimethyl sulfoxide (DMSO) has been used to prepare the concentrations of the compound (0.03, 0.06, 0.3 and 0.6 M) by the equation below (13).

$$\mathbf{C_1V_1 = C_2V_2}$$

where C_1= Concentration of stock solution, V_1= Volume acquired from a stock solution, C_2= Final concentration, V_2= Final volume. Ethylene glycol was utilized as a diluent solution.

Evaluation of antifungal property of ZnS:Mn Nanoparticles

The agar dilution technique has been used to evaluate the ready ZnS:Mn nanoparticles against fungi according to (22) and as reported below:

1- Different volumes from the prepared extracts have mixed separately with 100 ml of SDA (sterilized Sabouraud Dextrose Agar) with a view to prepare the wanted concentrations of these compounds for the test (0.03, 0.06, 0.3, 0.6 M). The mixture of compounds has been shaken enough, and then pours the mixture into petri dishes to solidify in sterilized conditions.
2- Size 8 mm of Piece from the mycelial growth of 15 days old mould culture was put in the middle of every plate. The incubation period of the inoculated plates was 7-10 days at 28°C. It has been doing replicates per treatment.

3- The changing in the diameter for the fungal colony was determined, after that, measuring of the growth inhibition can be calculated for the antifungal activity of every concentration using the following formulation (22,23).

Growth inhibition% = [[Growth in control - Growth in treatment]/Growth in control] ×100%

Statistical Analysis:

Analysis System-Microsoft SAS (2012) has been used to the statistical evaluation of the outcomes. The chi-square analysis was utilized to compare consequence between the growth inhibition rates.

Results and Discussion

a) X-ray diffraction (XRD) analysis

The XRD results indicate to, as shown in fig 1, that ZnS:Mn nanoparticles have been acquired in a powder shape. As clear from the XRD pattern, the broadened peaks indicate to forming small crystallites of ZnS:Mn nanostructures.

It is observed that there are three diffraction peaks of spherical nanoparticles ZnS:Mn at 2 Theta in positions 28.55°, 47.90°, 55.27° correspond to diffraction planes (111), (220) and (311) respectively. It found that the obtained results in agreement with reference (24).

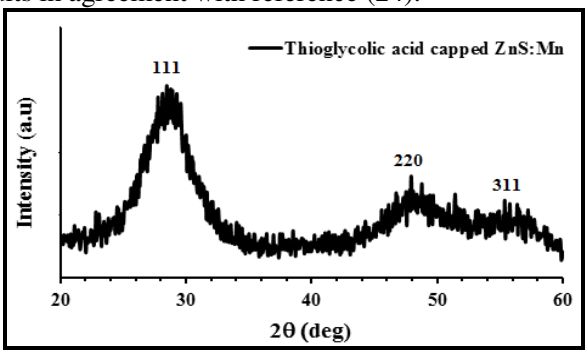

Figure.1 XRD pattern of ZnS:Mn nanoparticles synthesized by aqueous chemical method.

The calculation of the average size of crystalline (D) from (FWHM) of the peaks mention above can be evaluated by using the Debye-Scherrer equation

$$\mathbf{D = K\lambda / (\beta \cos \theta)}$$

where **D** is the crystallite size, **K** is the geometric factor (0.9), **λ** is the X-ray wave length (1.54 Å) for (Cu K_α), **β** is the full width at half maxima (FWHM) of the diffraction peak (in radian) and **θ** is the diffraction angle.

From the equation above, it was found that the average particle size has been determined to be 2.73nm. The d-spacing is estimated utilizing the formula (25);

$$\mathbf{(d_{hkl} = n\lambda / 2\sin\theta)}$$

From XRD results, in Fig. 1, it found that the lattice parameter and unit cell volume of $ZnS:Mn^{+2}$ nanoparticles equal to 5.4326 **Å** , 160.3392$Å^3$ respectively . The computed structural properties are presented in Table 2.

Table2. structural parameters of $ZnS:Mn^{+2}$ NPs.

2θ (degree)	Plane (hkl)	Interplaner Spacing d(A°)	Lattice Constant a(A°)	FWHM (rad)	Average Crystallite Size D(nm)	Dislocation Density δ(lines/m^2)

28.5501	(111)	3.12655		0.079		
47.9029	(220)	1.89904	5.4326	0.065	2.73	17.70×10^{16}
55.2795	(311)	1.66182		0.052		

The percentage of defects in the sample denoting to dislocation density (δ) can be computed using the following equation (25)

$$(\delta = 1/D^2)$$

b) FESEM analysis and EDS study

As shown in the Fig. 2 the FESEM results show that the ZnS:Mn nanoparticles have a spherical shape and obtained homogeneous and uniform distribution and roughly to an average diameter of around 30nm.

While in the Fig. (3) the EDS result shows that the atomic percentages of Zn and S were 51.88% and 48.12%, respectively, and had an atomic ratio of Zn:S = 1:0.92. Also the inset table of the Fig. (3) used to supporting that the ZnS:Mn nanoparticles have a good stoichiometric compound.

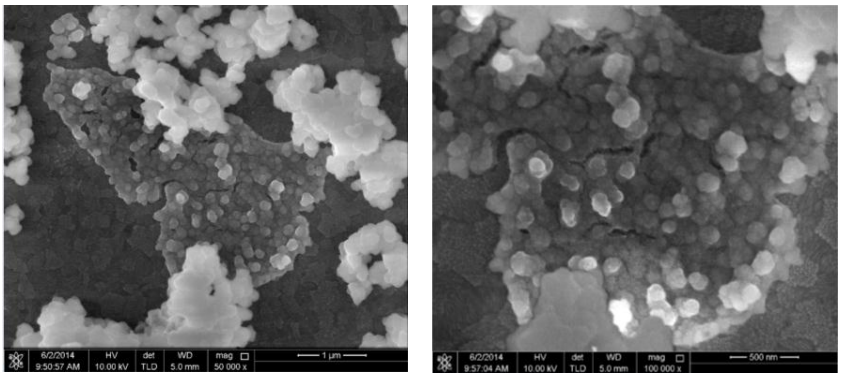

Figure 2. FESEM images of the synthesized TGA capped ZnS:Mn nanoparticles

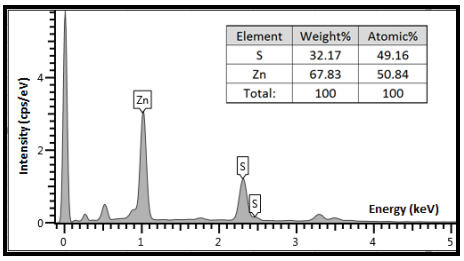

Figure 3. Chemical analysis through EDS of the prepared sample.

c) Absorption and band gap determination for colloids

UV-Vis absorption spectra of the synthesized TGA capped ZnS:Mn nanoparticles have been carried out to gauge the band gap. It has been found that these nanoparticles have a sharp absorption at wavelength 290 nm and that illustrates the essential absorption edge. This result is supported by (26). The kind and value of the optical band gap of the nanoparticles have been determined from the essential absorption edge, according to the excitation of the electron from the valence band to conduction band. It has been found that the spectrum of these particles has the absorption edge at 305 nm and these nanoparticles presence blue-shifted difference of bulk ZnS which has absorption edge at 345 nm as presented by (27). This shift in the absorption edge has been affected owing to diminution of the size particles also is imputed to the quantum confinement limit reaching of nanostructures, leading to an additional detached energy spectrum of the single nanoparticles (28). The band gap of the prepared nanostructured ZnS:Mn was specified using the Tauc's relation

$$[\alpha h\nu = A(h\nu - E_g)^m]$$

where A is a constant, which related with the type of material, α is the absorption parameter, h$\boldsymbol{\nu}$ is the energy of photon, E_g is refer to the band gap, and m refers to the kind of transmission. In this case, the exponent m equal to ½, owing to ZnS has a direct band gap energy which in agreement with previous studies (27, 29, 30). From the linear side of the diagram can be extrapolated that $(\boldsymbol{\alpha h\nu})^{1/m}$=0 to find the bandgap energy. Fig. 4 show the plot of TGA capped ZnS:Mn nanoparticles; (the inset is UV-Vis absorption spectrum).

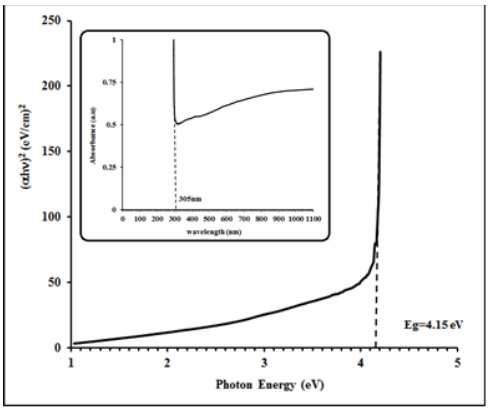

Figure 4. Tauc plot of TGA capped ZnS:Mn nanoparticles; (the inset is UV-Vis absorption spectrum).

From the results in Fig. 4, it found that the optical band gap of ZnS:Mn equal to 4.35 eV with a blue shift in the band gap about 0.75 eV which gives difference of bulk ZnS (3.60 eV). This indicating to occur a strong quantum confinement caused to reduce the particle size in nano range. The shift in the band gap with lessening size resulting from the confinement of an exciton in a limited sized crystalline can be qualified utilizing the model of "particle in a box".

For a spherical particle, Brus equation can be used to give a solution for this model, as the following equation (31):

$$\Delta E_g = E_{g(nano)} - E_{g(bulk)} = [\pi^2\hbar^2/2\mu r^2] - [1.8e^2/\epsilon \cdot r]$$

where ΔE_g refers to the blue shift of the band gap, μ is reduced mass, ħ is reduced blank constant. This gives the relation between the nanoparticle radius r, in nanometers, with the optical band gap E, in electron volt. While the parameters of the bulk ZnS are recognized, after substituting all the values of the parameters of ZnS in above equation, the particle's radius can be determined from the formula below (32):

$$r(nm) = \{-0.2963 + (-40.1970 + 13620/\lambda_p)^{1/2}\}/\{-7.34 + 2481.6/\lambda_p\}$$

The above formula, represents the crystal's radius (r) related with the peak absorbance wavelength (λ_p) for ZnS nanostructures which may have highly band gap energy owing to quantum confinement influence, gave a result equal to 2.88 nm which is in agreement with obtained result from XRD which is 2.73nm.

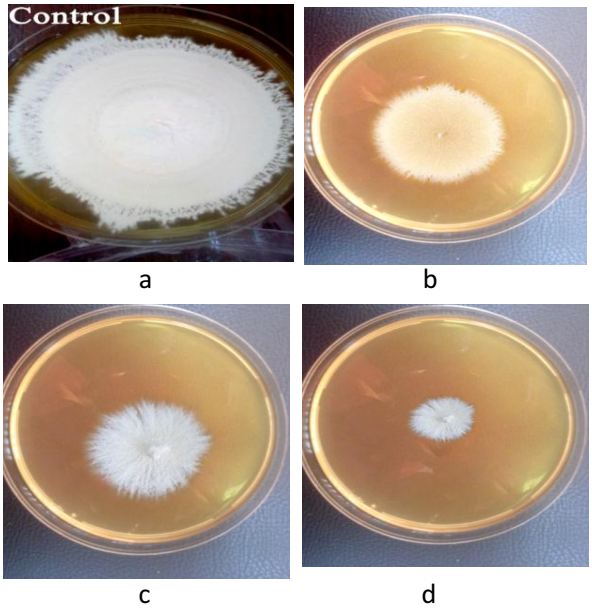

Figure 5. The effect of ZnS:Mn NPs on *M.audouinii* growth using Agar dillution methods; (a indicates the control, b, c and d indicates 10%, 20% and 30% dilluted NPs)

d) Inhibitory effects of ZnS:Mn nanoparticles on four kinds of fungus species

Inhibitory effects for different concentrations of ZnS:Mn nanoparticles against fungus are showed in Table (3). The inhibitory effects varied according to fungi species.

Table 3. Inhibition rate of TGA capped ZnS:Mn nanoparticleson different fungus species.

Fungus	Concentration (treatments) %			Chi-square–χ^2 value
	10 %	20 %	30 %	
Aspergillus fumigatus	51	77	100	9.462 **
Aspergillus falvus	30	73	92	10.702 **
Trichophyton mentagrophyte	37	62	87	10.538 **
Microsporum audonii	15	32	53	8.592 **
Chi-square–χ^2 value	8.307 **	10.299 **	18.762 **	-----

** (P<0.01).

In this study, it is obviously indicates that ZnS:Mn nanostructures synthesized by a simple aquatic chemical method using pure aqueous route resulting crystallite sizes of 2.73 nm. Debye – Scherrer formula has been used to calculate the crystallite size. FESEM technique has been used to investigate the morphology of the synthesized nanostructures.

The antifungal activity of ZnS:Mn NPs toward four fungal strains as samples for fungi was studied. In general, the inhabitation rate of TGA capped ZnS:Mn NPs was increased for all models of fungus with increasing of the nanoparticle concentrations as shown in Table (3). These results reveal that ZnS:Mn nanoparticles manifested a vigorous antifungal activity versus examined fungal strains. It was found that the maximum inhabitation rate was in Aspergillus fumigatus equal to (100) at 30% of concentration. While the minimum inhabitation rate was in *Microsporum audonii* equal to 53 at 30% of treatment. It is observed that at a 10% concentration most of the fungus have high resistant to the treatment more than 50% and the inhibition rate of antifungal particles very less in the samples. While during increase the concentration to be 20%, it found that the resistance to the treatment is decreased approximately to half in

some of the fungus, on the other side, the inhibition rate increased. 86% percentage of the fungus decreased their resistance to the treatment more than 50% by increasing the percentage of concentration to 30% and Fig. (5 to 8) illustrate the images of inhabitation for the four studied fungi.

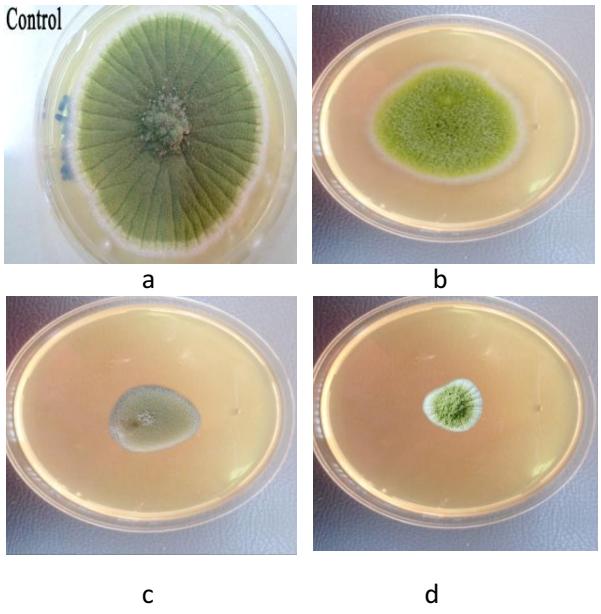

Figure 6. The effect of ZnS:Mn NPs on *Aspergillus flavus* growth using Agar dillution methods; (a indicates the control, b, c and d indicates 10%, 20% and 30% dilluted NPs)

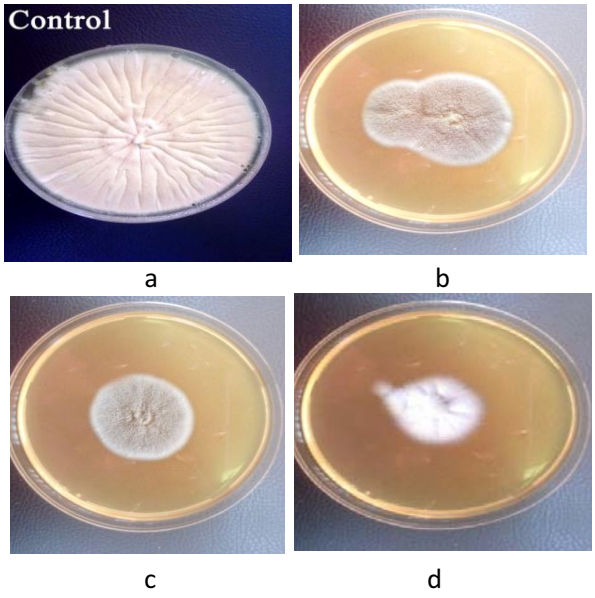

Figure 7. The effect of ZnS:Mn NPs on *Trichophyton mentagrophytes* growth using Agar dillution methods; (a indicates the control, b, c and d indicates 10%, 20% and 30% dilluted NPs).

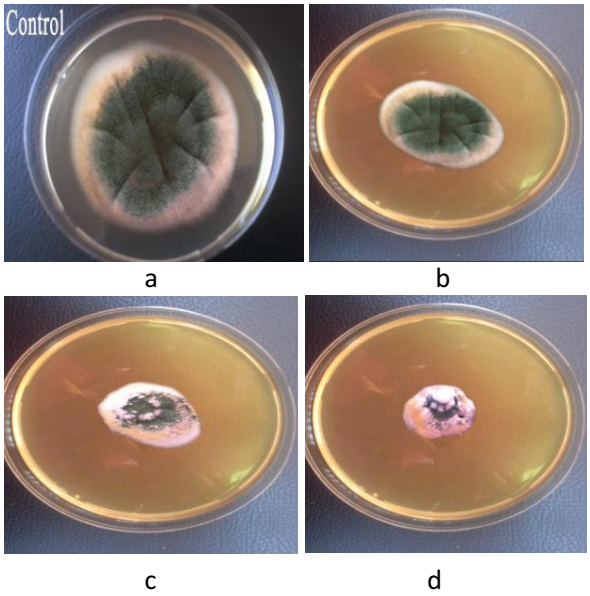

Figure 8. The effect of ZnS:Mn NPs on Aspergillus fumigatus growth using Agar dillution methods; (a indicates the control, b, c and d indicates 10%, 20% and 30% dilluted NPs)

The current study indicates ZnS:Mn NPs possess significant antifungal activity compare with other antifungal drugs. It was clear that there were factors for antimicrobial activity of nanostructures involved in the generation of reactive oxygen species (ROS) and efflux mechanisms resulting in releasing of constituent ions (27). Antifungal activity of ZnO NPs notified that the disruption of the cell membrane can be happened during the contact of the nanoparticles with cell membrane, this can be a factor of disruption of the cell membrane (28). As a result of connect the nanoparticles to the microbe cell membrane can affect the permeability of membranes and leading to oxidative stress preventing cell outgrowth (29) .

Previous studies showed that the greater antimicrobial activity can be achieved through smaller particle size (30, 31), therefore, the particle size can play a good role in addition to effect of increasing of the concentration. As suggested in (26, 32) that the doping can affect the crystallite of ZnS by reducing the size to be smaller. In this study, Doping with Mn gave average crystallite size equal to 2.73 nm as shown in Table (2). In the present investigation, the inhibition of antifungal property of ZnS:Mn which implemented without light radiation can be explained by creating electron-hole couples depending on ROS mechanism through its essential defects (Zn and sulphur). H^+ and OH^- ions can be producing them from the interaction of the holes with H_2O as well as superoxide radical anions produced from convert dissolved oxygen molecules by the electrons. Consequently, it can be produced hydrogen peroxide anions $HO2^-$ from transform HO_2 radicals which produced by reaction of H^+ with the superoxide radical anions. Therefore, the disruption of the fungal cell can be achieved by permeation of the peroxide to the cell membrane owing to oxidative stress (4, 33). In the status of ZnS:Mn nanoparticles, the existence of sulphur vacancies is the evident exporter of band transformations to generate H_2O_2. Also efflux mechanism suggested that the activity of Zn^{2+} ions can influence cell membrane by passing through the membrane and causing cell death. These mechanisms and the smaller size of nanoparticle which got from the doping by Mn supported ZnS:Mn caused irreparable harm affecting cell death and immediately affect the rate of inhibition which appears clearly in the results (34, 35).

Conclusions

In summary, it is the first study of an antifungal property of ZnS:Mn nanostructures prepared by chemical synthetic as against to four fungal models. Doping Mn with ZnS produced smaller nanoparticles size,

causing an increase in the inhibition rate during contact the nanoparticles with the cell membrane. Both of generation of hydrogen peroxide and presence of Zn^{2+} produced irreparable damage and cell death. ZnS:Mn NPs manifested as a potential antifungal factor can be applied to eliminate pragmatic infections.

References

1. H. Bai, Z. Liu, D. Sun. 2011. Hierarchical ZnO/Cu "corn-like" materials with high photodegradation and antibacterial capability under visible light. Phys. Chem. 13, 6205-6210.
2. Y. Lipovsky, A. Nitzan, A. Gedanken, R. Lubart. 2011. Antifungal activity of ZnO nanoparticles the role of ROS mediated cell injury. Nanotechnology, 22**,** 10, 105101.
3. E. Perelshtein, N. Ruderman, T. Perkas, J. Tzanov, E. Beddow, T. Joyce. 2013. ZnO-based complex nanoparticles: formation, characterization, and antibacterial activity. J. Mater. Chem. B. 1, 1968-1976.
4. N. Perkas, A. Lipovsky, G. Amirian, Y. Nitzan, A. Gedanken. 2013. Biocidal properties of TiO_2 powder modified with Ag nanoparticle. J. Mater. Chem. B. 1, 5309.
5. M. A. Nouri, M. M. Al-Halbosiy, B. I. Dheeb, A. J. Hashim. 2015. Cytotoxicity and genotoxicity of gliotoxin on human lymphocytes *in vitro*. J. King Saud Univ Sci. 27, 193–197.
6. G. Applerot, A. Lipovsky, R. Dror, N. Perkas, Y. Nitzan, R. Lubart. 2009. Enhanced Antibacterial Activity of Nanocrystalline ZnO Due to Increased ROS-Mediated Cell Injury. Adv Funct Mater. 19, 6, 842-852.
7. B. I. Dheeb. 2013. Immunohistochemical study of Tumor Necrosis Factor-alpha (TNF-α) expression in lung, liver, and spleen during aspergillosis infection. BMC genomics. 15, 2, 71.
8. J. Sawai, H. Igarashi, A. Hashimoto, T. Kokugan, M. Shimizu. 1996. Effect of Particle Size and Heating Temperature of Ceramic Powders on Antibacterial Activity of Their Slurries. J C E J. 29, 2, 251-258.
9. S. Nair, A. Sasidharan, R. V. Divya, D. Menon, S. Nair, K. Manzoor. 2009. Role of size scale of ZnO nanoparticles and microparticles on toxicity toward bacteria and osteoblast cancer cells. J Mater Sci Mater Med. 20, 1, 235-241.
10. I. I. Al-Mashhadani, B. I. Dheeb, E. N. Ismail, S. M. Majeed, D. M. Majeed. 2014. A Study of the Expression of Aflatoxin B1 Regulatory Gene in Clinical and Environmental Aspergillus flavus using Real-time PCR. IJSBAR. 17, 1, 417-427.
11. A. S. Haja, C. Karthikeyan, S. Sasikumar, K. V. Senthil, S. Kumaresan, G. Ravi. 2013. Impact of alkaline metal ions Mg^{2+}, Ca^{2+}, Sr^{2+} and Ba^{2+} on the structural, optical, thermal and antibacterial properties of ZnO nanoparticles prepared by the co-precipitation method. J. Mater. Chem. B. 1, 5950.
12. Z. H. Yang, C. Xie. 2006. Zn^{2+} release from zinc and zinc oxide particles in simulated uterine solution. Colloids Surf B Biointerfaces. 47, 2, 140-145.
13. A. R. Al-Tekreeti, M. M. Al-Halbosiy, B. I. Dheeb, A. J. Hashim, A. F. Al-Zuhairi. 2017. Molecular identification of clinical Candida isolates by simple and randomly amplified polymorphic DNA-PCR. Arab J. Sci Eng. 43, 1, 163–170.
14. G. Li, J. Zhai, D. Li, X. Fang, H. Jiang, Q. Dong. 2010. One-pot synthesis of monodispersed ZnS nanospheres with high antibacterial activity. J. Mater. Chem. 20, 9215-9219.
15. D. W. Synnott, M. Seery, S. Hinder, G. Michlits, S. Pillai. 2013. Anti-Bacterial Activity of Indoor Light Activated Photocatalysts, Appl Catal B. 130, 106-111.
16. J. Bang, R. Helmich, K. Suslick. 2008. Targeted Removal of Metallic Contamination from Lithography Solvents Using Membrane Purifiers. Advanced Materials. 20, 2599.
17. A. Nasrollahi, Kh. Pourshamsian, P. Mansourkiaee. 2011. Antifungal properties of silver nanoparticles on some of Fungi, Int.J.Nano.Dim. 1, 3, 233-239.
18. M. S. Ali-Shtayeh, S. I. Abu Ghdeib. 1999. Antifungal activity of plant extracts against dermatophytes, Mycoses. 42, 665–672.

19. S. Silver. 2003. Bacterial silver resistance: molecular biology and uses and misuses of silver compounds. FEMS Microbiol. Rev. 27, 341–353.
20. B. I. Dheeb, N. H. Al-Mudallal, Z. A. Salman, M. Ali. 2015. The Inhibitory Effects of Human, Camel and Cow's Milk against Some Pathogenic Fungi in Iraq. JJBS. 8, 2, 89 – 93.
21. I. M. Ali, I. M. Ibrahim, E. F. Ahmed, Q. A. Abbas. 2016. Structural and Characteristics of Manganese Doped Zinc Sulfide Nanoparticles and Its Antibacterial Effect against Gram-Positive and Gram-Negative Bacteria. Open J Biophys. 6, 1-9.
22. N. Al-Zoraky, K. Nakahara. 2003. Antibacterial activity o f extracts from some edible plants commonly consumed in Asia. Int J Food Microbiol. 80, 223-230.
23. SH. Mohammed, KM. Thalij, KI. Bander, BI. Dheeb. 2008. Survey Study of the Allergic Fungi in Kirkuk Area and Use Molecular Detection for Identification. IJSBAR. 19, 1, 383-397.
24. J. X. Yang, S. M. Wang, X. L, Zhao, Y. P. Tian, S. Y. Zhang, B. K. Jin, 2008. Preparation and characterization of ZnS nanocrystal from Zn(II) coordination polymer and ionic liquid. J Cryst Growth. 310, 19, 4358-4361.
25. M. Dhanam, B. Kavitha, S. Velumani. 2010. Structural and Characteristics of Manganese Doped Zinc Sulfide Nanoparticles and Its Antibacterial Effect against Gram-Positive and Gram-Negative Bacteria. Mat. Sci. Eng. B. 174, 209-215.
26. S. Y. Lee, Y. H. Shin, Y. Kim, S. Kim, S. Ju. 2011. Thermal quenching behavior of emission bands in Eu-doped ZnS nanowires. J. Lumin. 131, 7, 1336-1339.
27. B. S. Rema, R. Raveendran, A. V. Vaidyan. 2007. Synthesis and characterization of Mn2+-doped ZnS nanoparticles Pramana – J. Phys. 68, 4, 679-687.
28. J. K. Jaiswal, H. Mattoussi, J. M. Mauro, S. M. Simon. 2003, Long-term multiple color imaging of live cells using quantum dot bioconjugates. Nat. Biotechnol. 21, 47–51.
29. Z. Jindal, N. K. Verma. 2008. Photoluminescent properties of ZnS:Mn nanoparticles with in-built surfactant. J Mater Sci. 43,19, 6539–6545.
30. A. Ishizumia, C. Whiteb, Y. Kanemitsu. 2005. Photoluminescence properties of impuritydoped ZnS nanocrystals fabricated by sequential ion implantation. Physica E. 26, 1, 24–27.
31. L. E. Brus. 1984. Electron –electron and Electron-hole interaction in small semiconductore crystallites: The size dependence of the lowest excited electronic state, J. chem. Phys. 80, 9, 4403.
32. S. Shionoya, W. M. Yen, 2nd edit. 1999. Phosphor Handbook, Boca Raton, CRC Press, 169-170.
33. BI. Dheeb, M. M. F. Al-Halbosiy, R. K. Al lihabi, B. M. Khashman. 2016. The effects of Rubus idaeus extract on normal human lymphocytes and cancer cell line. BMC Genomics. 17, 6, 19.
34. F. El-Hilali, BI. Dheeb, BM. Traore, M. Messouak, H. Mazouz. 2016. Blood Transfusion Utility During Cardiopulmonary Bypass and Correlation with Key-Biochemical Laboratory Findings: A New Approach to Identify Preventive and Risk Factors (1-Year Practice at University Hospital Hassan-II of Fez). Biochem Anal Biochem, 5, 3, 1-6.
35. NJ. Abdulbaqi, BI. Dheeb, R. Irshad. 2018. Expression of Biotransformation and Antioxidant Genes in the Liver of Albino Mice after Exposure to Aflatoxin B1 and an Antioxidant Sourced from Turmeric (*Curcuma longa*). J J S, 11, 2, 89 – 93.